16th Australasian Fluid Mechanics Conference
Crown Plaza, Gold Coast, Australia
2-7 December 2007

Cylinder Wake – Boundary Layer Interaction in the Near Field

C. J. Dillon-Gibbons[1], C.Y. Wong[1], L. Chen[2] and J. Soria[1]

[1]Laboratory for Turbulent Research in Aerospace and Combustion
Monash University, Melbourne, Victoria, 3800 AUSTRALIA

[2]Department of Defence
Defence Science and Technology Organisation, Melbourne, Victoria, 3207 AUSTRALIA

Abstract

The interaction between the wake generated from separation off a cylinder and turbulent structures evident in a boundary layer are of significant importance in understanding the flows for cooling towers, submerged and semi-submerged vessels. This investigation was conducted on a wall mounted circular cylinder 25.4mm in diameter in the near wake region using MCCDPIV (multi-grid cross correlation digital particle image velocimetry) using a PCO4000 CCD array with full resolution of 4008 x 2672 pixels^2 per image. The investigation was conducted for ($Re_D \equiv DU / \nu$) of 3600 and 5400. It was seen in the mean after taking the ensemble average of the instantaneous results that a stagnation line was formed between x / D = 1 and 1.5 downstream of the cylinder. The region of the cavity wake was highly turbulent having the largest velocity fluctuations in this region. The shape of the stagnation line was also seen to change, where for the Re_D = 3600 the stagnation line position from the cylinder changed for a given height above the flat plate surface at y / D = 0.

Introduction

The complex 2D flow around a cylinder has been investigated extensively in the past because important engineering applications have been identified which could potentially be advanced through understanding this flow. The application of an infinite length cylinder with a single fixed end can be seen in applications such as plume motion behind stacks, aerodynamics of cooling towers and the drag on submerged and semi-submerged vessels.

Many investigations have been conducted over previous decades into how the wake structure behind a cylinder behaviours, and under what conditions these structures change [2, 3, 4, 11]. Before vortex shedding takes place a cavity flow (see figure 1) can be used to describe the near field of the cylinder wake where a stagnation point occurs some distance down stream of the cylinder, where inside this region the flow is circulated back towards the body along the centre line until it bifurcates at the cylinder. The flow then circulates into vortical structures that are propagated down stream. This process is a highly 3-dimenional flow where the fluid in the recirculation region must move out of the plane or continuity in the flow will not be preserved, see in figure 1.

The flow that is going to be discussed in this paper is from a wall-mounted cylinder, this flow represented in figure 2 has already been investigated in the past [8, 9]. This flow not only exhibits a wake formed solely from the cylinder as discussed earlier but combining this with the boundary layer flow being present on the surface of the wall, a horseshoe vortex is generated by the rotation in the boundary layer up stream of the cylinder. This horseshoe vortex separates from the boundary layer due to the adverse pressure gradient produced from the cylinder. These vortex structures then interact with the cylinder and the cavity wake discussed earlier and propagates downstream. The spanwise motion of this horseshoe vortex generates considerable out of plane motion in the centre line flow directly downstream of the cylinder, where the measurements are taken.

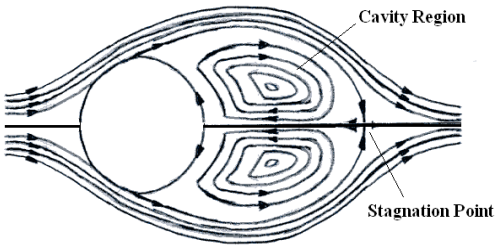

Figure 1: Idealised example of a wake cavity flow behind a cylinder figure adapted from [4].

The aim of this investigation was to observe the mean structures and the fluctuating velocity components in the near field, where the wake structure from a cylinder and a boundary layer interact by varying the Reynolds number.

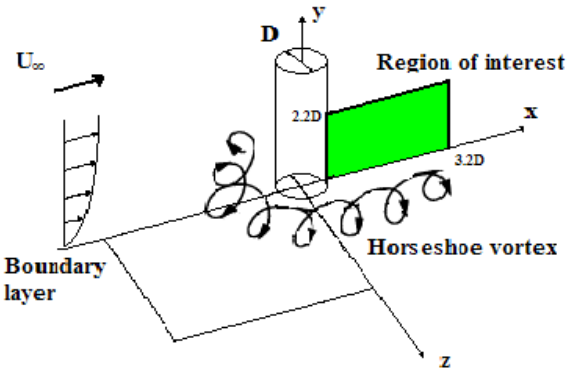

Figure 2: Sketch of vortical structures in flow around a wall-mounted cylinder showing coordinate system and region of interest for experiment.

Experimental technique and apparatus

Flow Geometry

The experiments were conducted in an open topped recirculating horizontal water tunnel at the Laboratory for Turbulence Research for Aerospace and Combustion (LTRAC). The tunnel has a 5.5m long working test section, split into 5 equal viewing windows regions of 1m length, with a cross-section of 500mm x 500mm.

The wake generating mechanism for this series of experiments was a circular cylinder of length, L = 600mm and diameter, D = 25.4mm. The cylinder was mounted vertically on a rigid plate

above the water surface of the tunnel with the base of the cylinder sitting flush on the floor of the working section of the tunnel. The base of the cylinder was padded in order to protect the perspex floor from scratches. By having the length of the cylinder longer than the height of the water, h = 480 mm the end effects from the cylinder were avoided and this in addition to the cylinder aspect ratio, L / D = 18.9 meant that the span-wise effects along the length of the cylinder were minimised. Any surface effects from the water tunnel have not been quantified and are to be addressed in ongoing experiments. The experiments were conducted in the centre line of the area downstream of the cylinder. The experimental layout and coordinate system can be seen in figure 2. The x-coordinate direction points in the direction of the free-stream where the velocity component is denoted by

$$u(x,y,t) = U(x,y) + u'(x,y,t) \tag{1}$$

such that

$$U(x,y) = \overline{u(x,y,t)} \tag{2}$$

Similarly the wall normal coordinate is y with its velocity component denoted by

$$v(x,y,t) = V(x,y) + v'(x,y,t) \tag{3}$$

such that

$$V(x,y) = \overline{v(x,y,t)} \tag{4}$$

The experimental conditions were chosen as U_∞ = 142 mm/s and 214 mm/s. These velocities gave Reynold Number Re_D ($\equiv U_\infty D$ / ν where ν is the kinematic viscosity of the water and U_∞ is the free stream velocity) = 3600 and 5400 based on the cylinder diameter. Under these conditions the boundary layer upstream of the cylinder can be specified from previous results in the same area of the LTRAC water tunnel as seen in reference [12]. Table 1 shows a summary of the important boundary layer specifications for the flow parameters in this paper.

Free stream Velocity, U (mm/s)	Displacement thickness, δ_1 (mm)	Momentum thickness, δ_2 (mm)	Shape factor, H_{12}
142	5.109	3.402	1.502298
214	4.125	2.785	1.481909

Table 1. Boundary layer specifications referenced from [12].

Particle Image Velocimetry

Particle image Velocimetry is a non-intrusive, optical velocity measurement technique in which the velocity field is measured indirectly by recording images of the light scattering tracer particles within in the flow. A plane of interest is illuminated by 2 successive pulses of a thin coherent light sheet (for this experiment by a laser) spaced a short pre-determined time apart. The light scatter from the tracer particles is then captured through a single exposure method for each of the two successive pulses on a CCD array. These two single-exposed images were then divided into regions known as interrogation windows (IW). A cross-correlation algorithm is then performed on each exposure over local IW. Using the known time delay between the two exposed images and each particles displacement in successive IW their individual velocities are then calculated. Further processing of the velocity data in two directions can also be calculated to extract more information, such as the vorticity of the flow field [5, 10].

Image Acquisition and Processing

The flow was seeded using 11um hollow glass spheres. These particles were illuminated using a laser light sheet produced by a frequency doubled dual-cavity New Wave Nd:YAG laser, 532nm. The acquisition apparatus used to capture the reflected light from the particles was a PCO 4000 CCD array with a full resolution of 4008 x 2672 pixels^2 per image. With an AF Micro Nikkor 200mm 1:4D lens set at an f-stop of 12. The PCO 4000 was positioned 450 mm from the plane of interest where the flow was measured (in the symmetry line of the cylinder wake). This corresponded to a magnification factor for the set of experiments being MF = 20.52 μm / px. This MF was check before and after each set of experiments to ensure that the camera was not moved and was always found to be within 0.05%. This MF corresponded to an area of interest through the CCD array of 82.25 x 54.83 mm^2 or 3.2D x 2.2D. Using this imaging arrangement 605 image pairs were taken for each tunnel velocity.

An in house multi-grid cross-correlation algorithm (MCCDPIV) [6] was used to analysis the data for each image pair. This was set using IW sizes of 32 x 32 px^2. The multi-grid option was then used to further reduce the IW down to a possible 24 x 24 px^2 with an overlap region of 50% or 12 px. With the current MF this corresponded to an IW of 0.66 x 0.66 mm^2 down to a multi-grid IW potential of 0.49 x 0.49 mm^2. A number of filtering tools were used to reject erroneous vectors from the displacement field. A Hart filter was employed using the 8 neighbouring correlation tables to the position in question, see [1], The maximum velocity ratio between two neighbouring position was set at 0.25. A dynamic mean value operator was used to check the mean displacement of the neighbouring points to the position of interest was within 0.001 over 3 standard deviations. A Chi square criteria along the closest 13 positions to the current position in the field was used to smooth the data.

Uncertainty analysis of the MCCDPIV algorithm by [7] found that the PIV displacement can be resolved to a precision of 0.1px with an uncertainty of 0.06px at a 95% confidence level. For these experiments this results in a single sample velocity uncertainty of 0.82mm/s. The velocity averages were calculated using 605 samples, which have an uncertainty of 0.065mm/s.

Instantaneous Results

Figure 3 shows two examples of instantaneous vector fields and streamlines resulting from the PIV analysis one for each of the experimental conditions described earlier. These vector fields only show every 8th vector as the high spatial resolution of the PCO4000 CCD array results in a very high density of vectors when analysed under the condition outlined above. The grey rectangle between x / D = 0 and 0.5 is the downstream half of the cylinder.

These instantaneous vector fields give us an indication of the accuracy with which we can represent the fluids motion in this area of the flow. These instantaneous plots show the highly turbulent nature of the flow seen in the centre line downstream of the cylinder in the near wake region. Figure 3(a) shows at least 3 sources, where the fluid moves in or out of the plane of the light sheet. Found in the vicinity of the cylinder where the 3 dimensional nature of the flow is highlighted. What can be seen in each of the instantaneous fields is that the flow is very turbulent directly downstream of the cylinder and then at approximately x / D = 1.5 the streamlines appear to exhibit a more settled motion. After this position the flow also appears to have a very distinct downward direction towards the boundary layer, although this is more pronounced in figure 3(b).

(a)

(b)

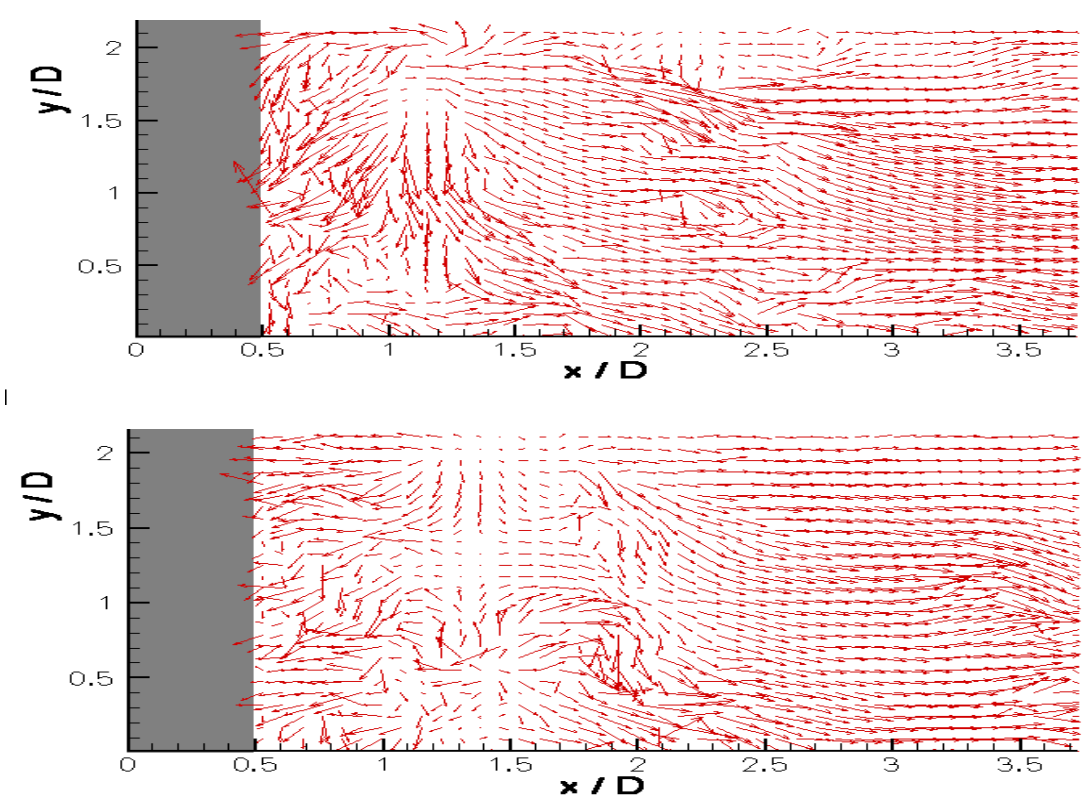

Figure 3: Instantaneous vector field showing every 8th vector for (a) Re_D = 3600 and (b) Re_D = 5400.

(a)

(b)

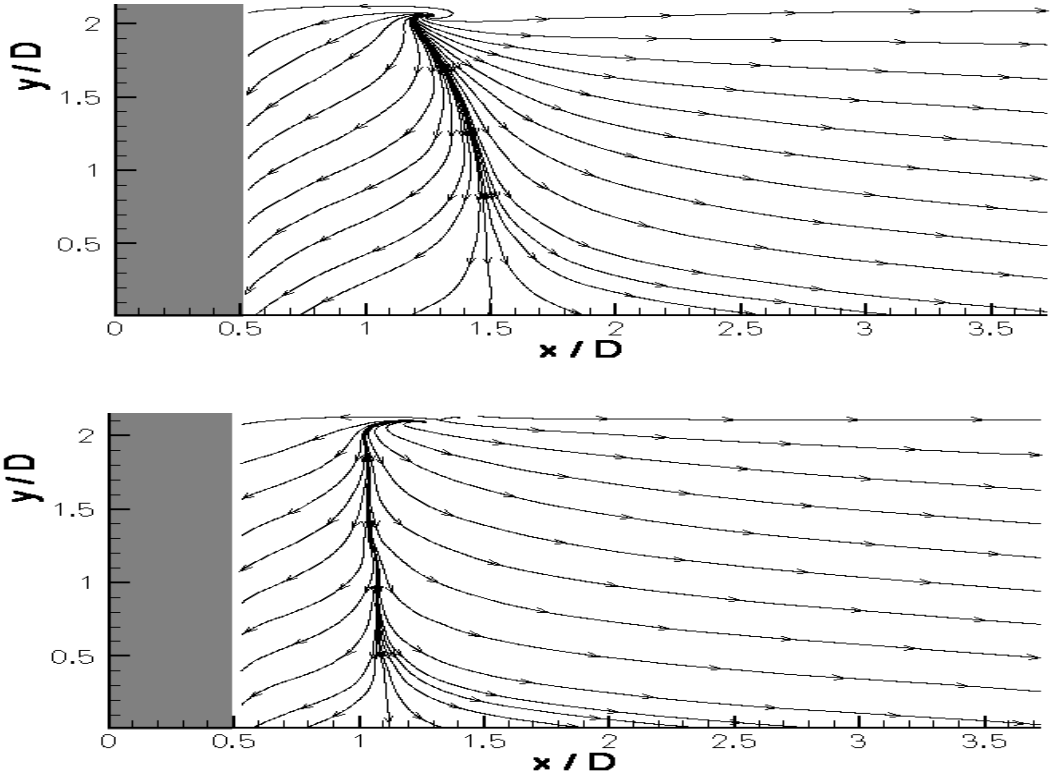

Figure 4: Ensemble averaged streamlines for (a) Re_D = 3600 and (b) Re_D = 5400.

Ensemble Averaged Results

The ensemble averaged results shown in figure 4 are from 605 instantaneous images for each case. What can be seen is that there is a very distinct stagnation line where the fluid flows back upstream towards the cylinder. This represents the length of the formation region which supports the notion of the cavity flow in the near wake proposed by [4] and which can be seen in figure 1. What is interesting to note is that for figure 4 (b) the stagnation line is constant at x / D ≈ 1.1. Except at y / D = 2.1 where the stagnation line bends downstream and becomes almost constant with y / D. In (a) the stagnation line curves from x / D = 1.5 at y / D = 0 to an interesting phenomenon at x / D = 1.3 when y / D = 2.0. The streamlines appear to originate from a stagnation point. These two stagnation line changing at high y / D values may be due to the close proximity off the edge of the viewing window of the CCD array. This may be verified by moving the viewing window up the length of the cylinder to include results past the current window height. This observation of the changing length of the formation region can easily be observed from figure 5. In figure 5(b) the velocity distribution down the centre of the cylinder wake collapses on top of one another until well downstream of the stagnation line. Whereas in figure 5(a) the lines are spread and differing values of stagnation line length from the cylinder can be observed. Despite the difference in stagnation line length the gradient of the velocity distributions for case (a) are relatively constant across y / D until well downstream of the stagnation zone, as is the case in (b). It can be seen that the length of the formation region is longer for the smaller value of Re_D.

(a)

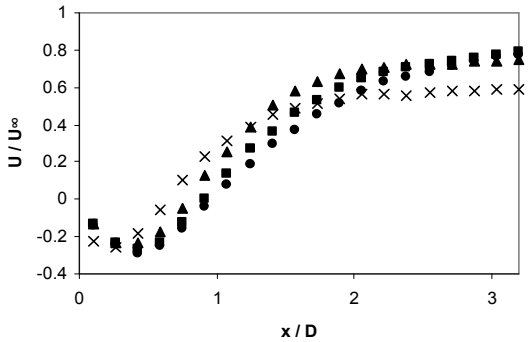

(b)

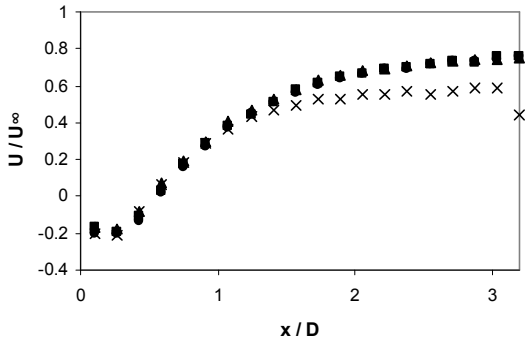

Figure 5: Velocity distributions, U / U_∞ for y / D = 0.5: ●, y / D = 1.0: ■, y / D = 1.5: ▲, y / D = 2: x, for the conditions (a) Re_D = 3600 and (b) Re_D = 5400.

It can also be seen from figure 4 that the downward motion that was identified downstream of the stagnation lines in the instantaneous fields (figure 3) is also present in the mean flow fields. It is also seen that there is a downward motion of the flow upstream of the stagnation line, this was not seen in the instantaneous fields as the flow was too chaotic to identify a general trend in this area of the flow.

Mean Velocities and Reynolds Stresses

It is interesting to note from figure 6 that the $\overline{u'^2}$ distributions show very similar trends between the two cases, with (b) Re_D = 5400 having a marginally higher peak value of $\overline{u'^2}$. However this peak in $\overline{u'^2}$ occurs in both cases upstream of the stagnation line where the flow is travelling towards the cylinder, against the direction of the free stream velocity. The values of $\overline{u'^2}$ then decline further downstream as x / D increases.
This shows higher velocity fluctuations in the x direction present in the vicinity of the stagnation line. This is consistent with current knowledge where large out of plane motion occurs for a cavity wake flow caused by the horseshoe vortices lapping around the cylinder from the boundary layer. Coupled with the out of plane motion of the eddy vortex structures shed from the boundary of the cylinder. The fluctuations then decline in the x direction as we travel further downstream away from the stagnation line showing a less turbulent and settling flow.

It can be observed from figures 7 that the $\overline{v'^2}$ fluctuations are again relatively consistent between the two cases except in the region of the stagnation line where the first case where Re_D = 3600 has a higher fluctuation in the y direction over the range y / D = 0 to 1.5. Similar to the $\overline{u'^2}$ fluctuations the $\overline{v'^2}$ fluctuations decrease as the flow progresses sufficiently far enough downstream of the stagnation line.

These higher $\overline{v'^2}$ fluctuation in the region of the stagnation line, as with the $\overline{u'^2}$ fluctuations will most likely be due to the highly unstable 3-dimensional flow that occurs due to the vortex structures generated from the cylinder and boundary layer.

Conclusions

The interaction between the wake from a cylinder and the boundary layer of a flat plate surface has been investigated. The Reynolds number for the undisturbed flow has been investigated for two conditions, Re_D = 3600 and Re_D = 5400 and the following can be concluded. In the mean a stagnation line occurs at a distance downstream of the cylinder variable with Re_D, The condition for Re_D= 5400 resulted in the stagnation line forming a shorter distance, approximately at x / D = 1 from the centre of the cylinder compared to a distance of x / D = 1 to 1.5 for Re_D = 3600. The shape of the stagnation line in the x-y plane also varied between the two cases with the higher Re_D flow resulting in a constant x / D position of the stagnation line for a given value of y / D, whereas the position of the stagnation line for Re_D = 3600 curved from x / D = 1.5 at y / D = 0 to x / D = 1 at y / D = 2.1. A definite downward motion towards the boundary layer was observed both upstream and downstream of the stagnation line in both cases. The velocity components in the x and y directions were highly unsteady in the region of the stagnation line, and even more so for low values of y / D, close to the boundary layer. This is most likely a result of the interactions and out of plane motion of the cavity wake from the cylinder and the horseshoe vortex generated from the flat plate in this region.

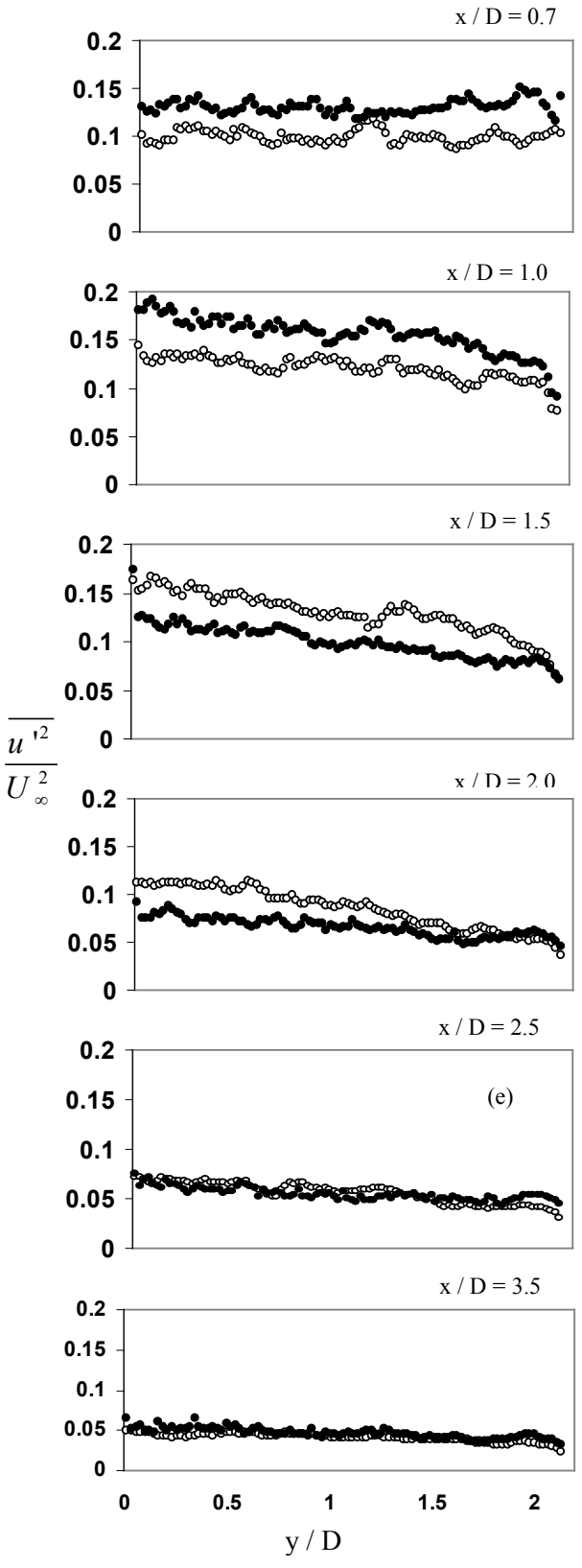

Figure 6: Spanwise variation of $\overline{u'^2}$ / U_∞^2, Re_D = 3600: ○, Re_D = 5400: ●.

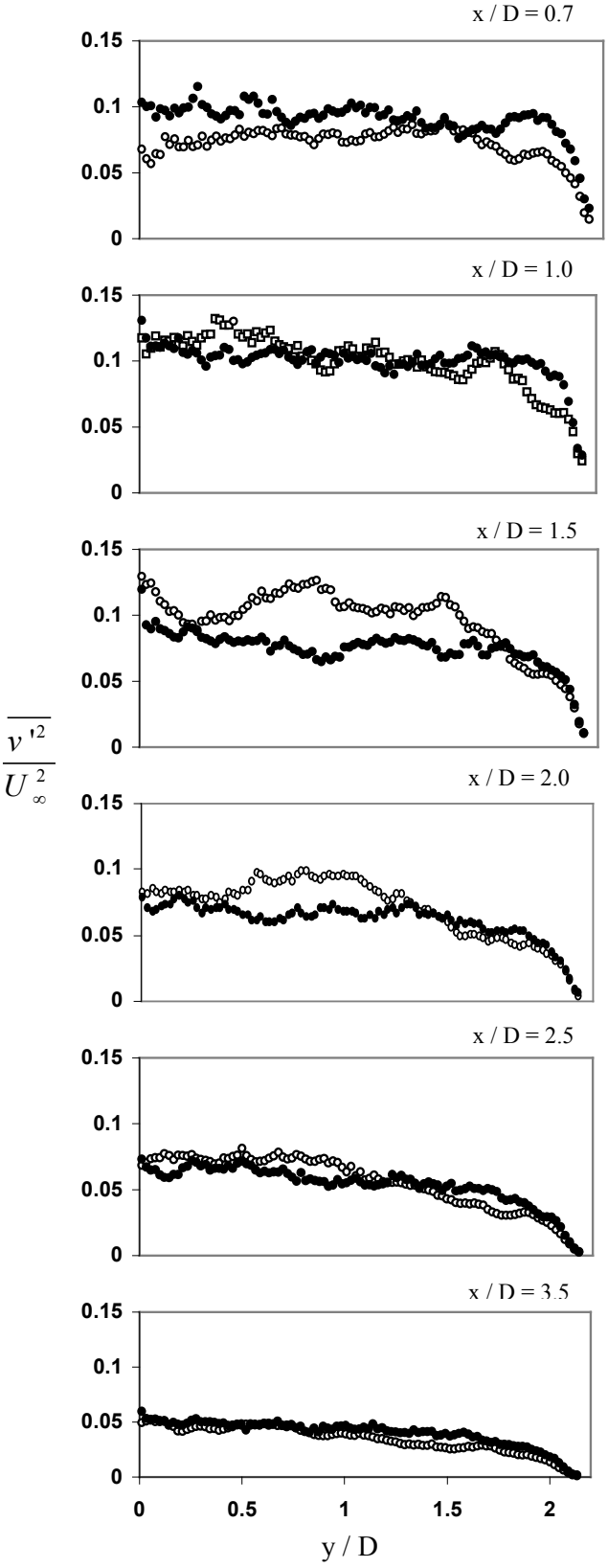

Figure 7: Spanwise variation of $\overline{v'^2}$ / U_∞^2, Re_D = 3600: o, Re_D = 5400: ●.

Acknowledgements

The authors gratefully acknowledge the support of the ARC. C.J. Dillon-Gibbons gratefully acknowledges the support from an Australia Postgraduate Award and a DSTO Postgraduate Top-up Scholarship to undertake this research.

References

[1] Hart, D.P., *PIV error correction*, Experiments in Fluids, **29**, 2000, 13-22.

[2] King, R., *A review of vortex-shedding research and its application,* Ocean Engineering, **4**, 1977, 141–171.

[3] Matsumoto, M., *Vortex shedding of bluff bodies: a review*, J. Fluids Struct. **13**, 1999, 791-811.

[4] Perry, A. E., Chong, M. S. & Lim, T. T., *The vortex-shedding process behind two-dimensional bluff bodies,* J. Fluid Mechanics, **116**, 1982, 77-90.

[5] Soria, J., Masri, A. & Honnery, D., *An adaptive Cross Correlation Digital PIV Technique for Unsteady Flow Investigations*, Proc. 1st Australian conference on Laser Diagnostics in Fluid Mechanics and Combustion, Sydney, Australia, 1996, pp. 29-45.

[6] Soria J., *Multigrid approach to cross-correlation digital PIV and HPIV analysis.* In Proceedings of the Thirteenth Australasian fluid mechanics conference, Monash University, Melbourne, 1998, 381–384.

[7] Soria J., *An investigation of the near wake of a circular cylinder using a video-based digital cross-correlation particle image velocimetry technique,* Experimental Thermal and Fluid Science, **12**, 1996, 221-233.

[8] Sumer, B.M., Christiansen N. & Fredsǿe, J., *The horeshow vortex and vortex shedding around a vertical wall-mounted cylinder exposed to waves,* J. Fluid Mechanics, **332**, 1997, 41-70.

[9] Wang, H.F., Zhou, Y., Chan, C.K., Lam, K.S., *Effect of initial conditions on interaction between a boundary layer and a wall-mounted finite-length-cylinder wake.* Physics of Fluids, **18**, 2006, 1-12.

[10] Willert, C.E. & Gharib M. *Digital particle image velocimetry,* Experiments in Fluids, **10**, 1991, 181-193.

[11] Williamson, C. H. K., *Vortex dynamics in the cylinder wake,* Annu. Rev. Fluid Mech. **28**, 1996, 477-539.

[12] Wong, C.Y. & Soria, J., *Characterisation of a Low Reynolds Number Turbulent Boundary Layer using PIV,* 16th Australia Fluid Mechanics Conference, Gold Coast, Australia, 2007.